Photoemission Study of Quantum Confinement Effects on Noble-Metal Nanofilms

Akinori Tanaka, Kazutoshi Takahashi, Masayuki Hatano, Koji Tamura, Shoji Suzuki, and Shigeru Sato

Department of Physics, Graduate School of Science, Tohoku University, Aoba-ku, Sendai 980-77, Japan

(Received: Jan. 30, 1997 Accepted: Feb. 19, 1997)

Abstract

We report here results from a photoemission study of Ag nanofilms with various thickness. In the valence band photoemission spectra, the intense peak has been observed just below the Fermi level, which is derived from the surface states in the *L* gap of Ag (111), and the additional fine-structures have been observed in the higher binding energy region than the surface states. It is found that the binding energies and the energy intervals of each peak change systematically as a function of the nanofilm thickness. It is considered that these additional fine-structures are originated from the quantum-well states derived from Ag *sp* valence bands. Furthermore, it is found that these quantum-well states can be observed within a binding energy region corresponding to the band structure mismatch between Ag (111) and Cu (111) substrate. We have also carried out the theoretical calculation based on the phase accumulation model which takes into account the phase shifts on reflections at both interfaces of Ag nanofilms. From a comparison of the experimental results with the calculated results, it is found that the spectral binding energy dependence on Ag nanofilm thickness is well characterized by phase accumulation model.

1. Introduction

Physical properties of nanostructures of solids have attracted much interest because they are expected to differ strongly from those of the corresponding bulk crystals. In a small nanocrystallite with a size in the range of a few nanometers to several tens of nanometers, low-dimensional confinement effects on electron-hole systems (quantum confinement effects) become predominant. Due to these effects, distinct physical properties (electronic structures, magnetic properties, transport properties, and optical nonlinear susceptibility, *etc.*) appear. Up to now, especially semiconductor nanostructures, such as semiconductor superlattices [1] and semiconductor clusters [2], have been studied fairy well both of theoretically and experimentally. On the other hand, the metallic nanostructures are recently also given attention from the viewpoint of applying them as magnetic recording devices, since it have been found that the multilayer structures composed of alternating ferromagnetic and nonmagnetic metals show the oscillatory magnetic coupling and the giant magnetoresistance (GMR) [3-5]. However, the research for the metallic nanostructures has been hindered by experimental difficulties, since most of experimental techniques developed for semiconductor systems are not applicable. In order to elucidate the intriguing properties of metallic nanostructures, it is indispensable to consider the low-dimensional confinement effect on the electronic structure in a metallic nanostructure.

In this work, we have carried out a photoemission study of Ag nanofilms with various thickness. Using molecular beam epitaxial (MBE) methods, Ag nanofilms were prepared on Si (111) 7×7 substrates by employing Cu films as seed layers. For the present Ag nanofilms, we observed the fine-structures in the valence band photoemission spectra, which are originated from the quantum-well states due to the confinement effects within Ag nanofilm. From a comparison of our experimental results with results of a calculation based on the phase accumulation model, which takes into account the phase shifts on reflection of the electron wave function at both interfaces of Ag nanofilms, we discussed the quantized electronic structures of Ag nanofilms in details.

2. Experiment

Ag nanofilms for photoemission measurements were grown by MBE methods using a JPS-100 (ANELVA Co.) MBE system connected directly to a ARUPS 10 (VG Scientific Co.)

photoelectron spectrometer. The base pressure of MBE system was in the 10^{-9} Pa range. We used Si (111) single crystals for the substrates. After chemical treatment by Shiraki's method [6], Si (111) single crystal wafers were introduced to the growth chamber of MBE system. Prior to film growth, Si (111) substrates were annealed around 850 °C under ultra-high vacuum (UHV) in order to obtain clean 7×7 reconstructed surface. Ag nanofilms were prepared using two processes suggested by Kingetsu *et al.* [7]. The first process was a growth of Cu seed layers on clean Si (111) 7×7 substrates. Cu with a thickness of 20 nm was deposited from 3 kW electron-gun evaporator onto Si (111) 7 × 7 substrate at room temperature, and then epitaxial Cu (111) layers were obtained. The second process was a growth of Ag nanofilms on Cu (111) seed layers. Ag was also deposited from 3 kW electron-gun evaporator onto 20 nm thick Cu (111) seed layer at room temperature. The deposition rates of Ag nanofilms were about 0.01 nm/sec monitored by a quartz thickness monitor. The cleanness and structure of deposited Cu and Ag films were checked by Auger electron measurement, reflection high energy electron diffraction (RHEED) and low energy electron diffraction (LEED) pattern. Both of Ag and Cu layers show the clear 1×1 diffraction pattern, indicating that Ag (111) nanofilms are epitaxially grown on Cu (111) seed layers. The thicknesses of Ag nanofilms were calibrated to within ±5 % by the results of *ex-situ* X-ray small angle diffraction measurements and *ex-situ* optical measurements.

The thus prepared samples were then transferred into the photoelectron spectrometer through the UHV chamber without exposure to air. The angle-resolved photoemission measurements were performed with He I resonance line ($h\nu$ = 21.2 eV) as the excitation sources at room temperature. The base pressure of the photoelectron spectrometer was better than 1-2×10^{-8} Pa. The total energy and angular resolutions were about 130 meV and ±2°, respectively. The photoemission spectra showed no change in the course of the measurements. The Fermi level of the sample was determined by comparison with a gold references.

3. Results and Discussion

Figure 1 shows the thickness dependence of the valence band photoemission spectra for Ag nanofilms. In the present system, Cu (111) seed layers act as the substrates supporting Ag (111) nanofilms. The photoemission spectra for the Ag nanofilms show the intense peaks just below the Fermi level. From the comparison with the results of photoemission studies for bulk Ag (111) clean surface [8-10], it is considered that these peaks just below the Fermi level are originated from the surface states located in the gap at the L point of the bulk Brillouin zone (see below). The photoemission spectrum for Ag nanofilm with a thickness of 13.0 nm is almost same as the previous valence band photoemission spectra for bulk Ag (111) clean surface [8-10], indicating that Ag nanofilm with a thickness of 13.0 nm exhibits similar electronic structure to bulk Ag (111). The sharpness of these surface states reflects the good crystallinity and crystal orientations of the present systems. The

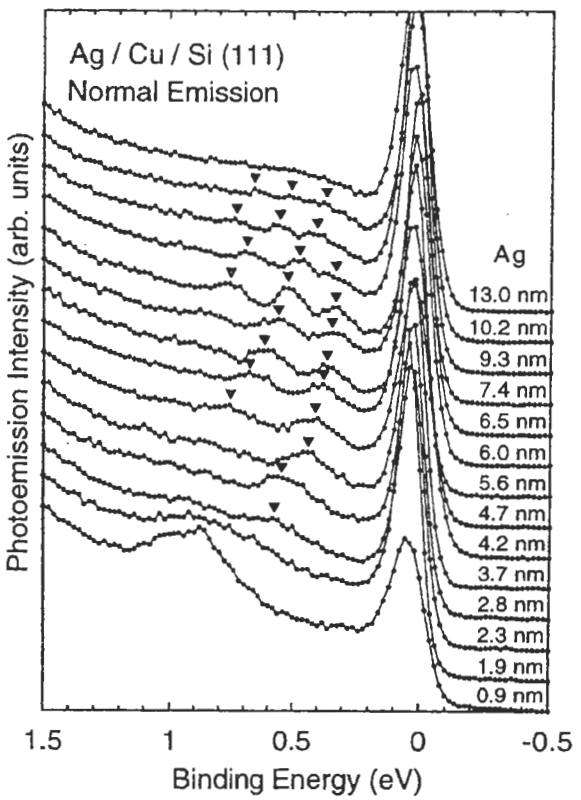

Fig. 1 Valence band photoemission spectra of Ag nanofilms measured with He I resonance line ($h\nu$ = 21.2 eV) at room temperature as a function of nanofilm thicknesses. Thicknesses of Ag nanofilms are indicated on each spectrum. The spectra were taken by a sample surface normal emission geometry. Solid triangles indicate the fine-structures originated from the quantum-well states.

photoemission spectrum for Ag nanofilm with the thickness of 0.9 nm shows the feature around 0.9 eV in binding energy, which is originated from a direct transition from Cu *sp* valence band as observed in bulk Cu (111) surface (not given in this paper), but the surface states around 0.4 eV observed for Cu (111) surface are completely disappeared. The contribution from Cu *sp* valence band also remain in the photoemission spectrum for the thickness of 1.9 nm.

In addition, the fine-structures are observed on the higher energy side than the surface states. In Fig. 1, these fine-structures are shown by solid triangles. As shown in Fig. 1, the binding energies and the energy intervals of each peak change systematically as a function of the nanofilm thickness. It is considered that these additional fine-structures are originated from the quantum-well states derived from Ag *sp* valence band (Λ_1 band), as previously reported for similar systems [11-13]. In the present system, the quantum confinement barriers are formed by Ag-vacuum and Ag-Cu interfaces. Therefore, the electron wave functions derived from Ag *sp* valence bands are confined within Ag nanofilms due to both interfaces and become the quantized electronic states in Ag nanofilm by the quantum confinement effects. As shown in Fig. 1, it is found that the quantum-well states can be observed up to a thickness of about 12.0 nm. However, it is difficult to discuss about the dimensional crossover on the electronic structures of Ag nanofilms, since the quantum-well states become too crowded to be resolved with our equipment.

In order to see more clearly the nanofilm thickness dependence of the peak energies of these quantum-well states, the binding energies are plotted as a function of the nanofilm thickness in Fig. 2. As shown in Fig. 2, it is found that four series of the quantum-well states are observed for the present systems. It is important to note that the quantum-well states are observed between about 0.3 and 0.9 eV in the binding energy. From the comparison with the valence band dispersion relations for bulk Ag (111) and Cu (111) along the [111] direction corresponding to Γ-L direction in the bulk Brillouin zone as shown in Fig. 3, these binding energies of about 0.3 and 0.9 eV correspond to the energies of $L_{2'}$ critical points in the bulk Brillouin zone for Ag and Cu, respectively. Therefore, the present quantum-well states are observed within a binding energy region corresponding to the band structure mismatch of Γ-L direction in reciprocal lattice space between Ag and Cu (the toned area in Fig. 3). For Ag *sp* valence electrons within a binding

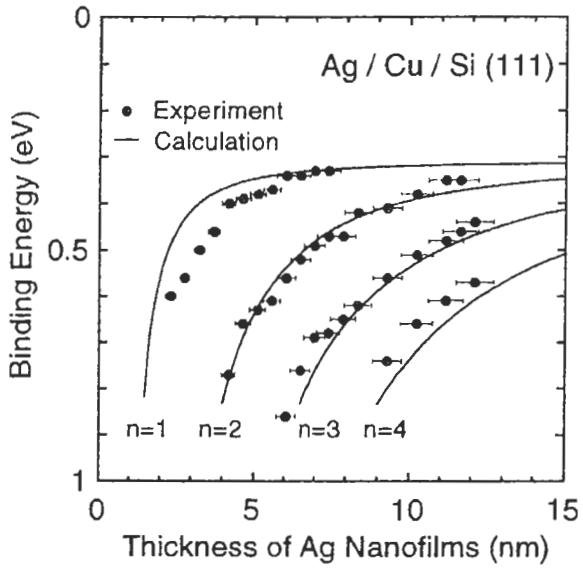

Fig. 2 Plot of the binding energies obtained from the valence band photoemission spectra for Ag nanofilms as a function of the nanofilm thickness (solid circles). The solid lines represent the calculated thickness dependence of the binding energy of the quantum-well states (with n = 1-4) for Ag nanofilms based on the phase accumulation model (see text).

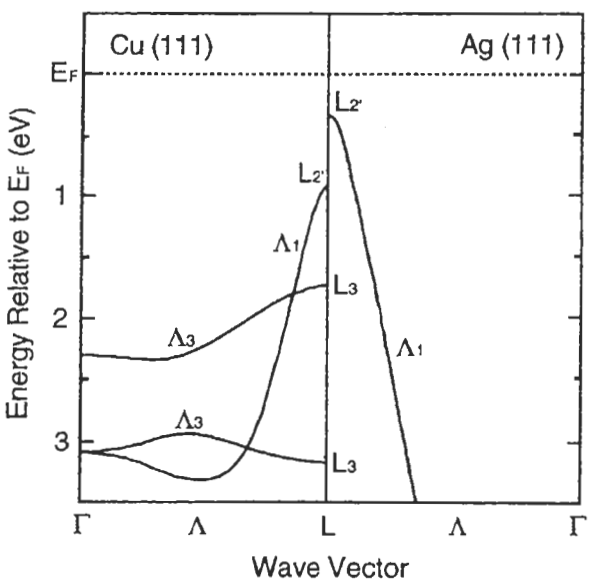

Fig. 3 Valence band dispersion relations for Ag (111) and Cu (111) along the [111] direction corresponding to Γ-Λ-L direction in the bulk Brillouin zone. The toned area indicates the binding energy region corresponding to the band structure mismatch of Γ-Λ-L direction in reciprocal lattice space between Ag and Cu.

energy region corresponding to the band structure mismatch, the electron wave function is forbidden for the propagation into Cu (111) substrates, since this energy region corresponds to the energy gap (L gap) region for Cu (111) substrate and then the energy conservation is not allowed for the transmission through Ag-Cu interface. Therefore, Ag *sp* valence electrons within the band structure mismatch region are confined within Ag nanofilm, and then the quantum-well states formed in Ag nanofilms. For Ag *sp* valence electrons outside the band structure mismatch region, the energy conservation is always allowed with Cu *sp* valence bands having the same energies, therefore, no quantum-well states are observed above about 0.9 eV in binding energy. This fact indicates that the quantum confinement effects on the present system rigidly occur due to the band structure mismatch between Ag (111) and Cu (111). On other hand, Mueller *et al.* [12] reported that the quantized electronic states were observed up to a binding energy of about 2.0 eV for Ag nanofilms grown on clean Cu (111) single crystal substrates. They interpreted that the electron reflection at the Ag-Cu interface can be significant due to less perfectly matched Ag-overlayer/Cu-substrate pairs and then the quantized electronic states were observed in the wide binding energy region as the quantum-well resonance for Ag nanofilms on Cu (111) single crystal surface. In conjunction with our present results, this means that the qualities of the interfaces between Ag nanofilms and Cu substrates for our samples are better than the previous systems, therefore, the present systems show the intrinsic quantum confinement effects determined from the electronic structures of Ag nanofilms and Cu substrates. In fact, the binding energies for present systems are slightly different from those for previous systems, and these differences may be originated from the differences of phase shifts on reflection of electron wave function due to the interface conditions.

In order to describe the quantum-well states theoretically, we consider the quantizations condition within the phase accumulation model which has characterized the image states and the surface states on clean surfaces [14, 15],

$$2kd + \Phi_C + \Phi_B = 2n\pi, \qquad (1)$$

where k is the electron wave vector components perpendicular to the surface, d is the nanofilm thickness, n is the quantum number, and Φ_C and Φ_B are the phase shifts on reflections of the electron wave function at Ag-Cu and Ag-vacuum interfaces, respectively. In Eq. (1), k is determined by the valence band dispersion along Γ-L direction of bulk Ag (111) shown in right hand side of Fig. 3, since the electron motions within the nanofilms is characterized by the same Hamiltonian as that for bulk Ag due to the short screening length. The dispersion relation along Γ-L direction of bulk Ag (111) based on the nearly free electron two-band model is represented by,

$$k(E) = k_L - (2m^* / \hbar^2)^{1/2} [(G + E) - (4GE + V_g^2)^{1/2}]^{1/2}, \qquad (2)$$

with $G = \hbar^2 k_L^2 / 2m^*$ and $V_g = 2.08$ eV is Fourier component of the crystal potential, where $k_L = 1.33$ A^{-1} is the Brillouin zone wave vector at the L symmetry point of Ag (111), $m^* = 0.74$ is the effective mass of electrons in this band. The above parameters reproduce the known band energies for bulk Ag (111). The phase shift on reflection of electron wave function at Ag-vacuum interface, Φ_B, is given by,

$$\Phi_B(E) = \pi [3.4 \text{ (eV)} / (E_V - E)]^{1/2} - \pi, \qquad (3)$$

where $E_V = E_F + 4.49$ eV is the vacuum level, which represents the phase shift for an image potential outside Ag nanofilm by using the WKB approximation [14-16]. The phase shift on reflection of electron wave function at Ag-Cu interface, Φ_c, is given by,

$$\Phi_c(E) = 2\arctan [k(E)^{-1}(p \tan(\pi/2+\delta) - q)], \qquad (4)$$

which is derived by introducing the wave function in Cu L gap with imaginary wave vector as $\Psi = \exp(qz) \cos(pz + \delta)$ [14, 17], and which reproduces the known band energies for bulk Cu (111). Using Eqs. (1)-(4), the energies for the quantum-well states with each quantum number n can be obtained as a function of nanofilm thickness d. In Fig. 2, thus calculated results of the binding energies with each quantum number n are shown by solid lines. As shown in Fig. 2, the experimental points of the peak binding energies agree with the calculated curves fairly well. It suggests that the energies of the quantum-well states by confinement within Ag nanofilms are well characterized by these phase accumulation model. This fact

means that the quantum confinement effects by the existence of Ag-Cu interface are rigidly originated from the band structure mismatch between Ag (111) and Cu (111), and that the electronic confinement effects by the existence of Ag-vacuum interface are described by a pure image potential. However, for Ag nanofilms with thin thickness region below about 3.0 nm, the agreement of the nanofilm thickness dependence (with n = 1) of the experimental data and the calculated result is poor, as shown in Fig. 2. It seems that the phase accumulation model is no longer valid for these thinner thickness region and that a more rigorous calculation such as tight binding calculations will be necessary for these thinner thickness region.

4. Conclusion

We have carried out a photoemission study for Ag nanofilms with various thicknesses. In the valence band photoemission spectra, the intense peak has been observed just below the Fermi level, which is derived from the surface states located in the gap at the L point of the bulk Brillouin zone of Ag (111), and the additional fine-structures have been observed in the higher binding energy region than the surface states. It is found that the binding energies and the energy intervals of each peak change systematically as a function of the thickness. It is considered that these additional fine-structures are originated from the quantum-well states derived from Ag *sp* valence bands. It is found that these quantum-well states can be observed within a binding energy region corresponding to the band structure mismatch between Ag and Cu. This indicates that the quantum confinement effects on the present systems rigidly occur due to the band structure mismatch between Ag and Cu and that the qualities of the Ag-Cu interfaces are better than the previous systems. We have also carried out the theoretical calculation based on the phase accumulation model which takes into account the phase shifts on reflections at both interfaces of Ag nanofilms. From a comparison of the experimental results with these calculated results, it is found that Ag nanofilm thickness dependence of the binding energies of quantum-well states is well characterized by phase accumulation model.

Acknowledgments

We thank the Ministry of Education, Science and Culture of Japan for financial support under Grant-in-Aids for Scientific Research.

References

1. See, for example, M. Jaros, *Physics and Applications of Semiconductor Microstructures* (Oxford Univ. press. Oxford, 1989).
2. See, for example, A. Tanaka, S. Onari, and T. Arai, Phys. Rev. B **45**, 6587 (1992), and references therein.
3. S. S. Parkin, Phys. Rev. Lett. **67**, 3598 (1991).
4. G. Binash, P. Grungerg, F. Saurenbach, and W. Zinn, Phys. Rev. B **39**, 4828 (1989).
5. M. N. Baibichi, J. M. Brote, A. Fert, F. Nuguyen Van Dau, F. Petroff, P. Eittenne, G. Creuzet, A. Friederich, and J. Chazelas, Phys. Rev. Lett. **61**, 2472 (1988).
6. A. Ishizaka and Y. Shiraki, J. Electrochem. Soc. **133**, 666 (1986).
7. T. Kingetsu and K. Sakai, J. Cryst. Growth, **137**, 633 (1994).
8. A. P. Shapiro, A. L. Wachs, and T.-C. Chiang, Solid State Commun. **58**, 121 (1986).
9. S. D. Kevan and R. H. Gaylord, Phys. Rev. B **36**, 5809 (1987).
10. T. C. Hsieh, P. John, T. Miller, and T.-C. Chiang, Phys. Rev. B **35**, 3728 (1987).
11. T. Miller, A. Samsavar, G. E. Franklin, and T.-C. Chiang, Phys. Rev. Lett. **61**, 1404 (1988).
12. M. A. Mueller, A. Samsavar, T. Miller, and T.-C. Chiang, Phys. Rev. B **40**, 5845 (1989).
13. F. Patthey and W.-D. Schneider, Phys. Rev. B **50**, 17560 (1994).
14. N. V. Smith, Phys. Rev. B **32**, 3549 (1985).
15. N. V. Smith, N. B. Brookes, Y. Chang, and P. D. Johnson, Phys. Rev. B **49**, 332 (1994).
16. E. G. McRae and M. L. Kane, Surf. Sci. **108**, 435 (1981).
17. P. M. Echenique and J. B. Pendry, Prog. Surf. Sci, **32**, 111 (1990).